Computers and Electronics in Agriculture 165 (2019) 104969

Contents lists available at ScienceDirect

Computers and Electronics in Agriculture

journal homepage: www.elsevier.com/locate/compag

Control system for a continuous compaction large square baler

Daniel E. Flick, Cyrus M. Nigon, Kevin J. Shinners*, Joshua C. Friede

Department of Biological Systems Engineering, University of Wisconsin, United Sates

ARTICLE INFO

Keywords:
Baler
Controls
Density

ABSTRACT

Bale density impacts the cost to harvest, aggregate, store and transport hay or biomass. To achieve legal transport weight limits in many countries, the large square bale (LSBe) wet basis density should be approximately 240 kg·m^{-3}. Current large-square balers (LSBers) create density by employing a reciprocating plunger to apply pressures in excess of 700 kPa to the bale face, but densification by a reciprocating plunger is inefficient because of the intermittent manner that the pressure is applied. What is explored here is an alternative bale densification method that uses an auger and conical compaction rollers to compact material in a continuous fashion. Compared to conventional LSBers, this new baler concept has the potential to create high-density bales with a machine that is less complicated and lighter weight. An important component of this baling mechanism was a closed-loop control system developed to achieve a desired bale density, as well as control bale separation and bale length. The control system varied bale chamber compression panel pressure to alter auger force and subsequent bale density. Using this control system enabled the baler to achieve dry basis densities ranging from 166 to 334 kg·m^{-3} with auger forces less than 44 kN, nearly a fifteen-fold reduction in force compared to a conventional plunger type LSBer.

1. Introduction

The large-square bale (LSBe) is currently the most common package for harvesting and storing commercial hay and biomass feedstocks. Bale density has been identified as the most sensitive biomass supply chain parameter because the efficiencies of aggregation, handling, storage, and transport are all related to bale density (Kenney et al., 2014; Shah and Darr, 2016). The most economical transport of biomass feedstocks occurs when legal weight limits of the transport vehicle are achieved (Searcy and Hess, 2010; Miao et al., 2013). To achieve legal weight limits in many countries, the wet basis load density should be approximately 240 kg·m^{-3} (Miao et al., 2013). However, this LSBe density goal can be difficult to achieve when baling many biomass crops and LSBer energy requirements increased exponentially with achieved bale density (Shinners and Friede, 2018).

After almost four decades of improvements, the conventional LSBer design is now highly optimized, but densification by a reciprocating plunger remains inefficient. The inefficiencies of the LSBer are inherent to the nature of the intermittent compression cycle. Each new portion of crop fed into the bale chamber is defined as a flake, and LSBes are usually made up of 35 to 50 flakes depending on actual bale length and density. The volume of one flake of material is compressed during approximately 10% of the plunger's total cycle time resulting in substantial peak force and torque loads, requiring a robust and expensive drivetrain (Siebenga, 2013). The energy requirements of compressing material in this intermittent fashion are large because of the combination of large peak compression forces, the relatively short duration and high frequency at which these forces are applied, and the additional large forces required to accelerate and decelerate the massive plunger. This research investigated the control system needed for an alternative baler concept that replaces the intermittent reciprocating plunger with a continuous feed auger and conical compression rollers.

2. Auger baler description

The design objective of the auger baler (ABer) was to achieve high-density LSBes using continuous, rather than intermittent, compaction (Sibley and Sibley, 1995). It was hypothesized that compaction in this manner would produce high-density bales with less force so that a simpler, lighter weight and less expensive high-density baler could someday be realized. The ABer had six key functional components (Fig. 1, Table 1).

Harvested material gathered by the pick-up was first transferred to the feed rotor and then to the front of the auger barrel. The auger flights then conveyed material toward the conical compacting rollers at the end of the auger. The auger and rollers laid material on the face of the

* Corresponding author at: 460 Henry Mall, Madison, WI 53706, United States.
E-mail address: kjshinne@wisc.edu (K.J. Shinners).

https://doi.org/10.1016/j.compag.2019.104969
Received 13 June 2019; Accepted 18 August 2019

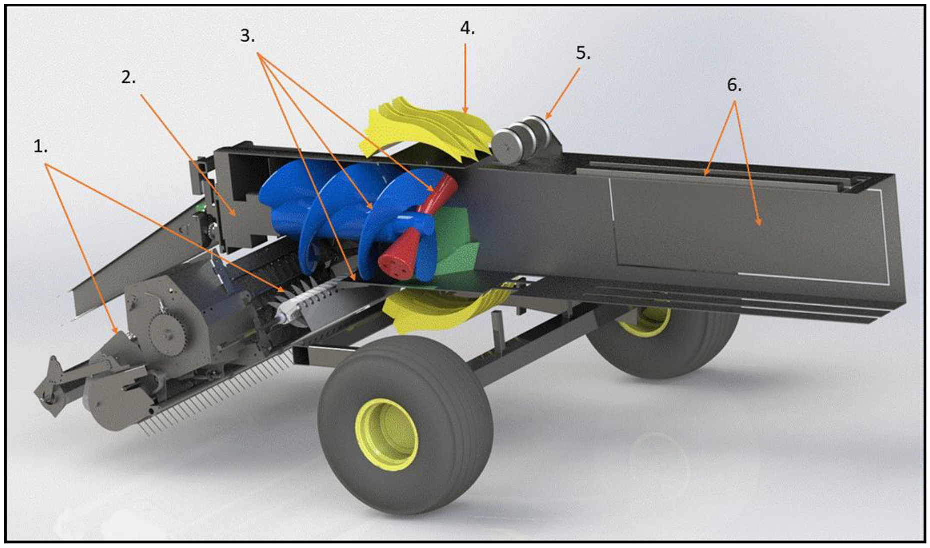

Fig. 1. Schematic cutaway of the auger baler showing: (1) pick-up and feed rotor; (2) auger gearbox; (3) auger, auger barrel, and conical compaction rollers; (4) bale separation system; (5) knotters; and (6) square bale chamber with converging compression panels.

Table 1
Relevant specifications of continuous compaction auger baler and conventional intermittent reciprocating plunger baler with comparable bale chamber cross-sections.

	Auger Baler	Conventional Baler[a]
Bale chamber cross section (cm)	76 × 76	80 × 89
PTO input speed (rev/min)	540 or 1000	1000
Gearbox reduction ratio	6:1	20 to 22:1
Compaction auger speed (rev/min)	90 or 167	None
Plunger frequency (strokes/min)	None	45–50
Flywheel mass (kg)	None	200–300
Converging bale chamber	Three-sides	Three-sides
Compaction system	Continuous	Intermittent
Timed components	Knotter system with separation arms.	Pre-compression system and knotter system with plunger.
Knotters	4 - Single Knots	4 - Double Knots
Baler height (m)	< 2.0	2.5–3.0
Baler mass (kg)	5500	7700–8500

[a] Typical values for most large square balers currently available and roughly of comparable size to the auger baler.

bale while continuously compressing the mat of material. The rollers had a relatively small "line-contact" area with the bale face, so high compaction pressures were applied with relatively low forces on the rollers and auger. The combination of rolling action with the relatively high applied pressures was intended to plastically flatten the crop stems, resulting in high-density bales. The auger chamber was cylindrical with stationary flights to assist in uniformly filling the barrel and to help move the material rearward. Angled diversion plates at the exit of the barrel were used to direct material to the bale chamber corners as a means to transition and distribute the crop material from the round auger barrel to the square bale chamber.

When the reciprocating plunger is at the furthest rearward position in a conventional LSBer, material in the bale chamber is separated from the incoming material in the pre-compression chamber. Activation of the knotter system when the plunger is in the rearward position completes the bale when the desired length is reached (McAfee et al., 2018). With the continuous compaction ABer there is no similar intermittent separation of the stream of material, so a mechanism was required to sever the continuous mass of material exiting the auger barrel and

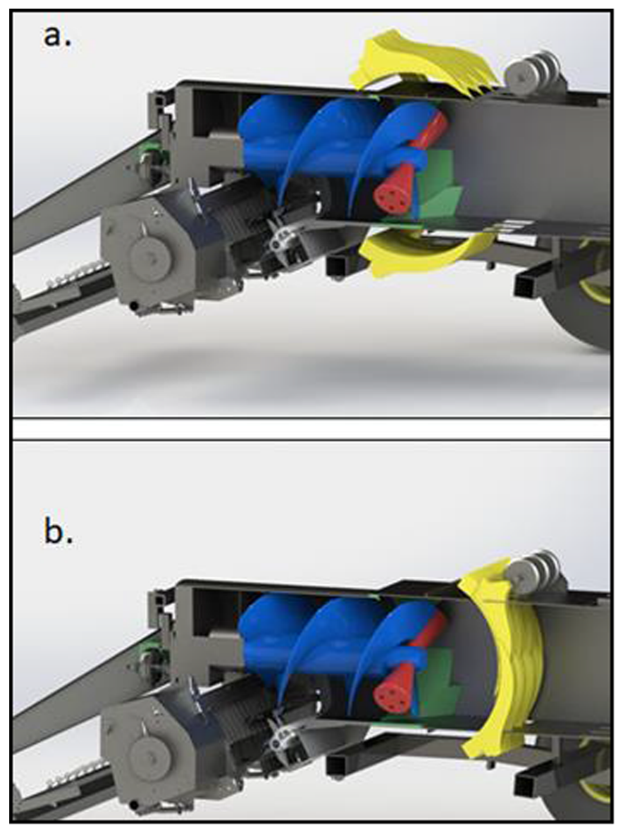

Fig. 2. Cutaway view of bale separation arms (yellow) at the home (a) and closed (b) positions. Note the space between the auger rollers (red) and the bale separation arms. Material accumulates here during bale separation and tying. (For interpretation of the references to colour in this figure legend, the reader is referred to the web version of this article.)

entering the bale chamber (Fig. 2). When the desired bale length was reached, the separation arms were hydraulically actuated to sever the material and create space for the knotter needles to bring twine around the trailing face of the bale to the knotters, thus completing the bale.

Similar to a conventional LSBer, the role of the ABer converging bale chamber compression panels was to create resistance to crop flow so that material densification would occur. This restriction was achieved by converging the chamber cross section on three sides, thus increasing the normal force on the sides of the bale which resulted in greater frictional resistance to material movement. Conventional LSBers use a control system where plunger force is used as a surrogate measure for bale density and hydraulic pressure in the compression panel convergence cylinders is used to control plunger force. To achieve a desired bale density, the operator chooses a target plunger force, often expressed as a fraction of the maximum force allowed by the control system, and the control system seeks to maintain that plunger force (Shinners and Friede, 2018). A similar density control system was needed for the ABer. Therefore, the objective of this research was to develop an ABer control system that would manage key machine systems and components to achieve a desired bale density and length. An additional objective was to use the control system during baling and iteratively change the control system parameters to improve its performance.

3. Control system development

The functional requirements of the developed system were to measure and control auger force, bale length, separation arm timing, knotter timing and compression panel hydraulic cylinder pressure. The control system was split into two separate functions – control of the compression panel pressure to alter bale density by maintaining a desired auger force, and control of the bale separation system when a desired bale length had been reached.

To facilitate machine operation, measurement of auger force, compression panel hydraulic cylinder pressure and bale length were required. Auger force was measured with a Digi-Star (Fort Atkinson, WI) model SBS-15 K load cell (67 kN capacity) mounted to the front of the auger gearbox mounting flange. Most of the auger force caused by bale compression was absorbed through the auger gearbox and gearbox mounting flange, so only a fraction of the auger force was transmitted to this load cell (Fig. 3). A calibration was performed by loading the auger through a separate load cell and hydraulic cylinder and measuring subsequent auger load cell force. The ratio of auger force to the load cell output was 8.46:1 with an R^2 of 0.999 (Flick, 2018). The load cell RS 232 signal was processed using a Digi-Star EZ-III indicator and then sent at 10 Hz to the baler control system for control and data collection purposes. Compression panel hydraulic cylinder pressure was measured by a diaphragm pressure transducer (model 02588676, maximum pressure 185 bar, Hydac Technology, Glendale Heights, IL). A conventional bale length star wheel was configured with a Koyo Electronics (Tokyo, Japan) model TRD-N500-RZWD rotary encoder to measure bale length. Separate limit switches were used to indicate the state (home or active) of the twine needles and the separation arms.

Compression panel hydraulic pressure was adjusted through a control loop to achieve a target auger force (Fig. 4). The control program performed two main functions: setting and controlling the auger force and controlling the compression panel convergence through changes to the cylinder pressure. The control was implemented using an Arduino (Turin, Italy) Nano microcontroller board which utilized an ATmega328P microcontroller. The microcontroller was programmed in C and compiled for the AVR architecture of the microcontroller (CodeVisionAVR C Compiler; Leuven, Belgium). The program consisted of nested (or cascading) proportional, integral, derivative (PID) loops. The control program considered the difference between actual and target auger force and provided the compression panel hydraulic pressure setpoint as the first output. In the second loop, this pressure setpoint was then compared to the current pressure measurement and then provided a pulse-width modulated (PWM) signal which was sent to the pressure reducing valve to achieve the target hydraulic pressure. The PWM valve was integrated into a valve block which also had an unloading valve to facilitate manual bale ejection, a maximum pressure relief valve (14.0 MPa), and the pressure transducer (Fig. 5). The PWM valve was essentially a pressure relief valve with a variable pressure setting. The maximum compression panel hydraulic cylinder pressure setpoint was limited to 13.8 MPa to prevent damage to hydraulic components.

A separate control loop programmed into the same microcontroller was used to attain the desired bale length and finish the bale by activating the separation arms and the twine knotter system (Figs. 5 and 6). When the desired bale length had been reached, the controller sent a signal to a solenoid valve, actuating the separation arm hydraulic cylinders. When the hydraulic cylinders were fully extended, a cam on the separation arm linkage mechanically actuated the knotter clutch, initiating twine needle movement, completing the bale by tying the twine knots. As the arms entered the bale chamber, material from the auger would push against the bale separation arms and auger force would rise (see results section). Since it was desired for the compression panels not to react to a change in force that did not impact the density of the bale in the chamber, the auger force control loop was paused until the separation and tying processes were complete. When the needles reached the home position, the separation arms were retracted, and the auger force control loop resumed when the separation arms returned to the home position (Fig. 6).

An Arduino Mega 2560 microcontroller board which utilized the ATmega2560 microcontroller was used to provide access to variables that could be adjusted through an interactive display in the tractor cab. This controller and display allowed changes to the bale length, compression panel, and auger force setpoints and to the PID control parameters. The three PID gain values for both pressure and force control

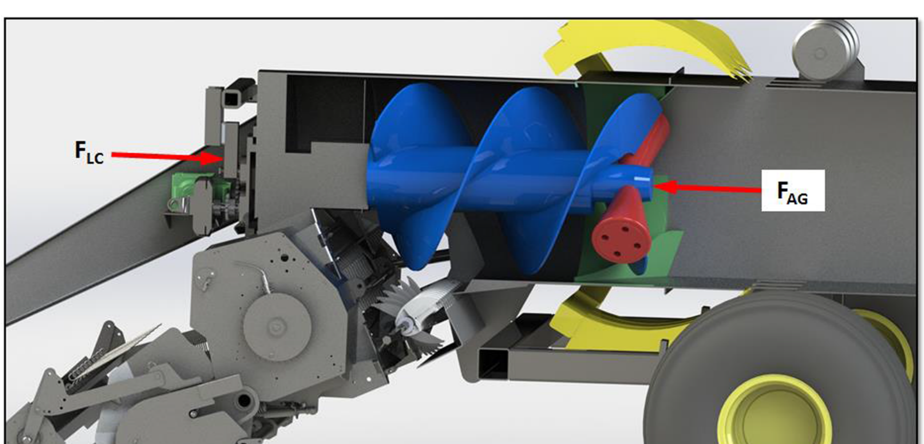

Fig. 3. Cutaway view showing the force on the auger load cell (F_{LC}) and the force (F_{AG}) at the end of the auger. Calibration found the ratio of auger force to the measured load cell output was 8.46:1 (Flick, 2018).

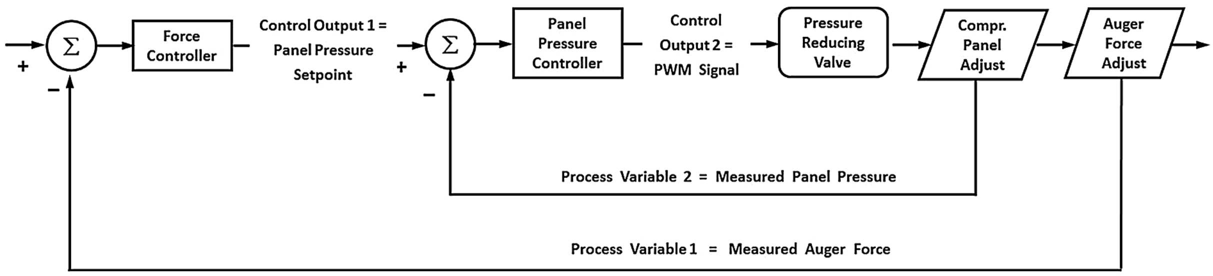

Fig. 4. Schematic of control loop used to control auger force through adjustment and control of compression panel cylinder hydraulic pressure.

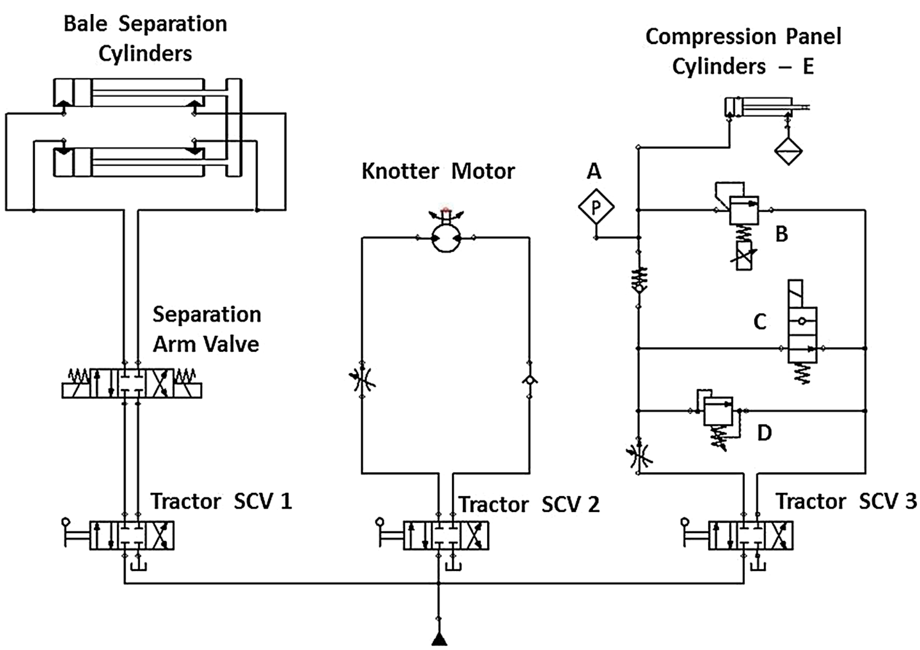

Fig. 5. Schematic of hydraulic system with (A) compression panel pressure transducer; (B) pulse width modulated pressure relief valve; (C) pressure unloading valve to facilitate manual bale ejection; (D) maximum pressure relief valve; and (E) compression panel cylinders (two removed for clarity). The system used tractor supplied hydraulic oil through one of three separate selective control valves (SCV).

could be set on the display for tuning purposes. A manual operating mode was available that allowed fixed settings of auger force or compression panel hydraulic pressure. This mode was used for tuning PID terms or for diagnosing baler performance issues. The display system also allowed the output of process data via USB. SerialPlot V0.9 (Ozderya, 2017) software was used to interpret, plot, and record the data directly to an Excel file.

The main function of the control system was to control auger force. Quantification of the performance of the control system was made by considering the absolute error between the setpoint and the auger load cell force signal output:

$$AE(i) = \frac{|SP - SO_i|}{SP} \tag{1}$$

where AE is the absolute error at each data point i; SP is the parameter setpoint; and SO_i is the auger load cell signal output. The average of the absolute error was then calculated to complete the evaluation of the system performance while baling. The PID terms for the auger force and the compression panel pressure controllers were tuned separately using the manual operational mode. Each system was tuned by first setting the PID terms, observing how the system responded when baling, and then iteratively adjusting the terms to achieve the desired system responsiveness. The system response around the desired setpoint was recorded and displayed in real time using the SerialPlot program. As each PID term was adjusted, the response was observed, and the acceptability of the response was based on the absolute error (Eq. (1)).

4. Materials and methods

A John Deere (Moline, IL) 6R series tractor with infinitely-variable-transmission (IVT) supplied tractive power, mechanical power through the power-take-off (PTO), and hydraulic power for ABer (Fig. 7). The compression panels, knotter assembly, and the bale separation system were powered by tractor hydraulic system (Fig. 5). The tractor's PTO powered the auger, crop pick-up and feed rotor (Fig. 1).

Before baling commenced, the bale length and auger force setpoints were entered into the control system. Then the hydraulic and PTO systems were actuated, the tractor was put in forward gear and baling would start. Varying the IVT ratio allowed the desired ground speed to be attained while maintaining a constant engine speed so PTO and auger speed could be constant. The bale was formed continuously at a selected auger force setpoint until the bale length setpoint was reached. Then the control system automatically closed the separation arms, actuated the knotter, and finally opened the separation arms once the bale had been tied.

To determine how well the control system functioned at various auger force setpoints and throughputs (i.e. ground speeds), an experiment was conducted when baling switchgrass, reed canarygrass, fescue, corn stover, and wheat straw. Preliminary tests in each crop helped determine which ground speeds and auger force setpoints to use as the experimental conditions. The maximum level of either variable was based on the tendency for the baler to plug. The minimum levels were based on subjective evaluation of adequate bale shape and density. An attempt was made to conduct the experiment at two levels of both ground speed and auger force. However crop availability, weather, or

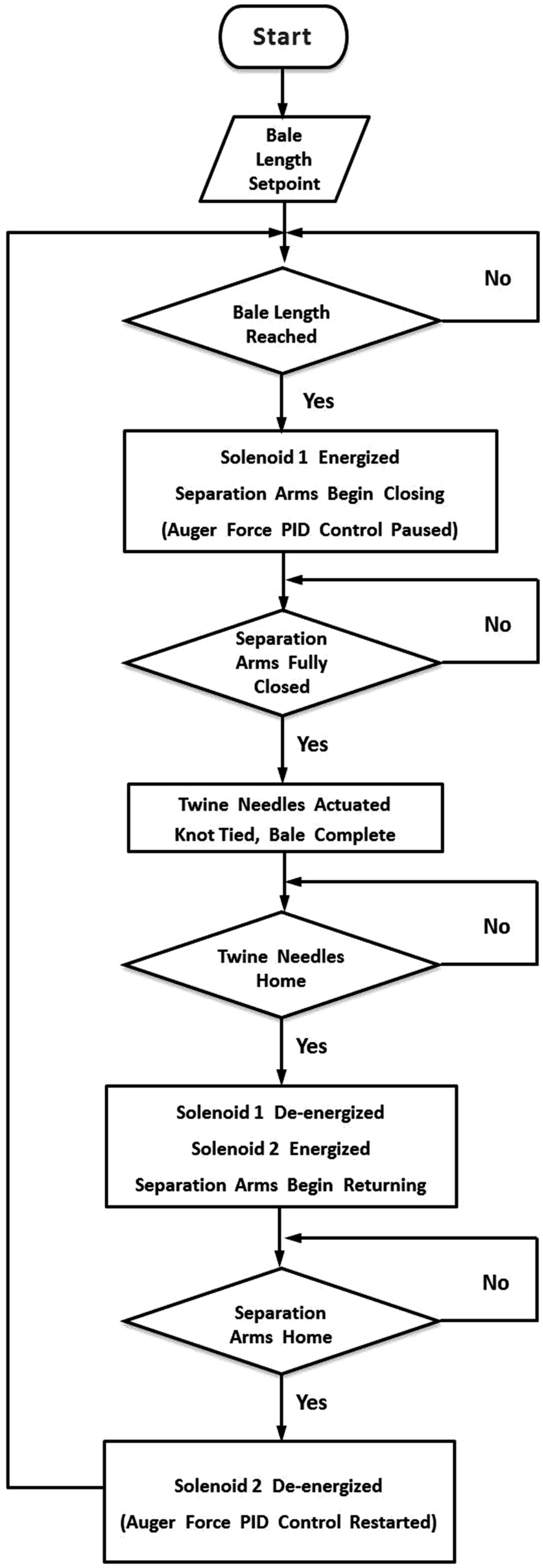

Fig. 6. Control loop for actuating the bale separation arms and twine knotter system when desired bale length had been reached.

Fig. 7. John Deere 6R tractor with auger baler baling fescue grass (top) and an example of the bales made with this baler (bottom).

mechanical breakdowns sometimes limited the extent of the variable levels actually tested. After baler equilibrium was reached for a given experimental condition, data collection then commenced for at least four replicate bales.

Results from the first experiment showed that for a given auger force, bale density decreased as throughput increased (see below). It was hypothesized that at greater throughputs each auger revolution placed a thicker layer of material on the bale face, so the auger force was less effective at compressing the material. Therefore, a second experiment was conducted to determine if increasing the auger speed could improve bale density at greater throughputs. This experiment was conducted using switchgrass, reed canarygrass, fescue, and wheat straw. Auger speed was changed by operating the tractor PTO at either 540 or 1000 rpm which resulted in auger speeds of 90 or 167 rpm, respectively. Two levels of ground speed were used to alter throughput and auger load cell force setpoint was maintained at 3550 N for all crops.

After both experiments, bale density was quantified by first weighing the bales on an 1800 kg capacity platform scale with a resolution of 0.5 kg. Relevant bale dimensions were then determined by hand measurement to the nearest 2 cm. Each bale was sampled at two locations to a depth of approximately 80 cm using a boring tool with 50 mm diameter. Samples were dried for 24 h at 103 °C according to ASABE Standard S358.3 (2012) for moisture content determination. Statistical differences between experimental conditions were determined using a least significant difference (LSD) at 5% significance level. The statistical analysis was conducted using an analysis of variance in the Data Analysis package in Excel.

5. Results and discussion

The developed control system was effective in controlling the auger force and bale length (Fig. 8). During continuous baling, the start of a bale was assumed to occur when the separation arms were fully retracted from the bale chamber (i.e. in the home position). At this point the auger force would drop due to the void left by the retracting arms (Fig. 8, A). The control loop was reactivated when the arms reached their home position, so the drop in auger force then caused the

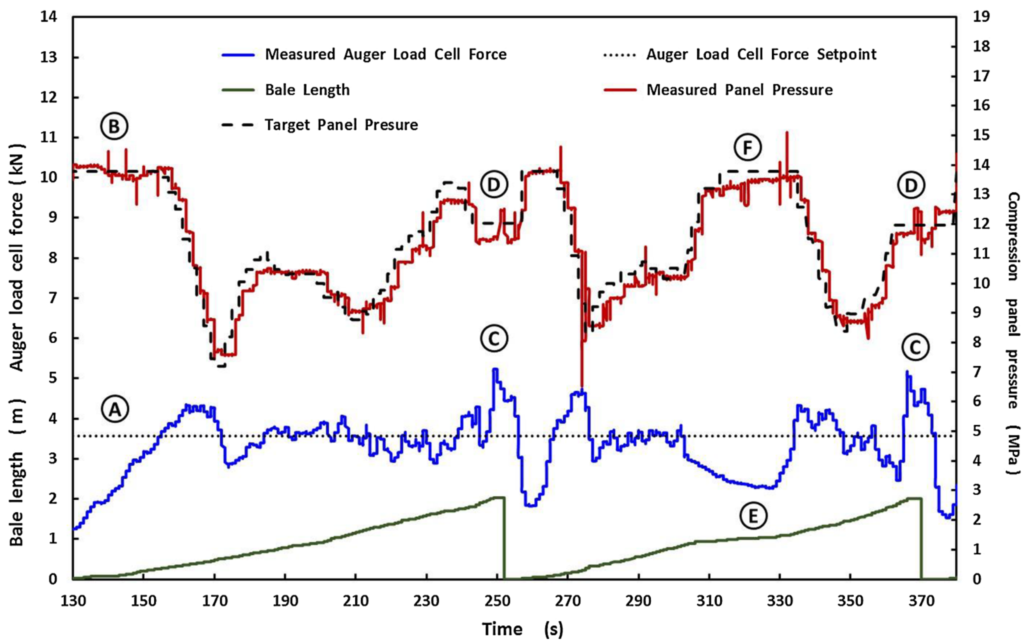

Fig. 8. Baler control system performance when baling fescue. Auger force was 8.46 times auger load cell force. Point A is the decrease in auger force immediately after the separation arms leave the bale chamber and point B is the reaction of the compression panel hydraulic cylinder pressure to the decreased force. Points C show the rise in auger force as material compacts against the separation arms when the bale is being separated and tied and points D show the compression panel control system paused at this time. Point E shows the drop in auger force during headland travel when no new material is being collected and point F the reaction of the compression panel to this decreased force.

Table 2
Auger baler performance using various auger load cell force setpoints and ground speeds during the first experiment. Auger speed was 90 rpm.

Auger Load Cell Force Setpoint (N)	Ground Speed ($km \cdot h^{-1}$)	Throughput[a] ($Mg \cdot h^{-1}$)		Bale Density[a] ($kg \cdot m^{-3}$)		Auger Load Cell Force[b] (N)		Auger Load Cell Force Error[b] (%)	
		Ave.	SEM	Ave.	SEM	Ave.	SEM	Ave.	SEM
Switchgrass[c,d]									
2,220	3.2	10.6 c	0.7	158 d	1	2,080 c	43	6 ab	2
3,550	3.2	13.4 b	0.3	180 b	3	3,448 ab	9	3 b	0
4,450	3.2	10.6 c	1.0	198 a	7	3,740 a	322	16 a	7
2,220	4.0	13.8 b	0.6	150 d	4	2,299 c	103	6 ab	4
3,550	4.0	14.1 b	0.7	169 c	6	3,146 b	229	13 a	6
2,220	5.6	20.6 a	1.4	151 d	3	2,271 c	66	4 b	2
LSD[e] (P = 0.05)		2.0		10		400		10	
Reed Canarygrass[c,d]									
2,220	3.2	12.1 b	1.9	171 c	2	1,898 b	33	15 a	1
4,000	3.2	11.1 b	0.3	225 a	5	3,531 a	77	12 a	2
4,000	6.4	14.4 a	0.9	202 b	4	3,376 a	153	16 a	4
LSD[e] (P = 0.05)		2.2		14		248		6	
Fescue[c,d]									
2,890	3.2	6.4 b	0.2	186 b	4	2,732 c	24	6 b	1
3,780	3.2	7.1 ab	0.3	195 b	5	3,424 b	24	9 ab	1
4,450	3.2	7.9 a	0.4	211 a	3	3,895 a	76	12 a	2
LSD[e] (P = 0.05)		0.8		11		131		3	
Corn Stover[c,d]									
3,340	2.4	6.2 d	0.3	180 b	2	2,887 c	75	13 a	2
4,230	2.4	7.2 c	0.3	190 a	4	3,887 a	46	8 b	1
3,340	4.8	10.6 a	0.3	163 c	5	2,855 c	43	14 a	1
4,230	4.8	9.4 b	0.5	180 b	1	3,724 b	42	12 ab	1
LSD[e] (P = 0.05)		0.9		9		141		4	
Wheat Straw[c,d]									
2,220	4.8	5.5 c	0.2	141 d	2	2,162 d	35	3 a	2
3,110	4.8	7.0 b	0.3	164 b	3	3,044 c	57	3 a	2
4,000	4.8	7.8 b	0.2	181 a	3	3,879 a	34	3 a	1
2,220	9.6	9.9 a	0.5	121 e	3	2,082 d	64	6 a	3
3,110	9.6	10.1 a	0.7	151 c	6	2,931 c	36	6 a	1
4,000	9.6	10.5 a	0.4	164 b	1	3,706 b	89	7 a	2
LSD[e] (P = 0.05)		1.0		8		132		4	

[a] Throughput and bale density reported on a dry basis.
[b] Auger load cell force averaged over the duration of each bale formed. Auger force was 8.46 times load cell force. The error of the auger load cell force was calculated using Eq. (1).
[c] Average wet basis moisture contents were 15% (switchgrass), 11% (reed canarygrass), 12% (fescue), 17% (corn stover), and 8% (wheat straw).
[d] Number of replicate bales per treatment was four for all crops.
[e] Least square difference. Averages in columns within each crop with different letters are significantly different at 5% significance level.

Table 3
Auger baler performance using various auger rotational speeds and ground speeds during the second experiment. Auger load cell force setpoint was 3,550 N.

Auger Speed (rpm)	Ground Speed (km·h^{-1})	Throughput[a] (Mg·h^{-1})		Bale Density[a] (kg·m^{-3})		Auger Load Cell Force[b] (N)		Auger Load Cell Force Error[b] (%)	
		Ave.	SEM	Ave.	SEM	Ave.	SEM	Ave.	SEM
Switchgrass[c,d]									
90	4.5	8.8 c	0.4	184 c	4	3,450 b	39	3 ab	1
90	7.1	13.1 b	0.4	169 d	2	3,567 b	125	6 ab	2
167	4.6	8.1 c	0.3	220 a	1	3,475 b	20	2 b	1
167	7.4	14.5 a	0.6	198 b	3	3,805 a	87	7 a	2
LSD[e] (P = 0.05)		1.2		7		201		4	
Reed Canarygrass[c,d]									
90	4.9	10.4 b	0.7	199 c	3	3,433 a	81	4 a	2
90	7.8	15.6 a	1.0	187 d	2	3,574 a	45	2 a	1
167	4.8	9.1 b	0.5	236 a	4	3,421 a	61	4 a	2
167	7.8	14.8 a	2.4	208 b	2	3,421 a	34	4 a	1
LSD[e] (P = 0.05)		3.6		8		153		4	
Fescue[c,d]									
90	3.3	6.6 c	0.4	233 b	7	3,470 a	27	2 b	1
90	4.9	13.2 a	0.7	196 c	3	3,521 a	72	4 ab	1
167	3.2	7.5 bc	0.4	270 a	6	3,422 a	32	4 ab	1
167	4.8	9.3 b	1.6	245 b	5	3,458 a	75	5 a	1
LSD[e] (P = 0.05)		2.4		15		142		2	
Wheat Straw[c,d]									
90	3.3	6.7 d	0.6	179 c	6	3,540 b	35	1 a	1
90	4.8	9.7 c	0.6	156 d	1	3,648 a	42	3 a	1
167	3.3	8.4 c	0.5	215 a	5	3,615 ab	28	2 a	1
167	4.6	12.1 b	0.3	189 b	4	3,599 ab	29	1 a	1
167	6.4	14.2 a	0.6	170 c	2	3,464 c	42	3 a	1
LSD[e] (P = 0.05)		1.5		9		75		2	

[a] Throughput and bale density reported on a dry basis.
[b] Auger load cell force averaged over the duration of each bale formed. Auger force was 8.46 times load cell force. The error of the auger load cell force was calculated using Eq. (1).
[c] Average wet basis moisture contents were 9% (switchgrass), 11% (reed canarygrass), 17% (fescue), and 11% (wheat straw).
[d] Number of replicate bales per treatment were 5 (switchgrass, fescue and wheat straw) and 4 (reed canarygrass).
[e] Least square difference. Averages in columns within each crop with different letters are significantly different at 5% significance level.

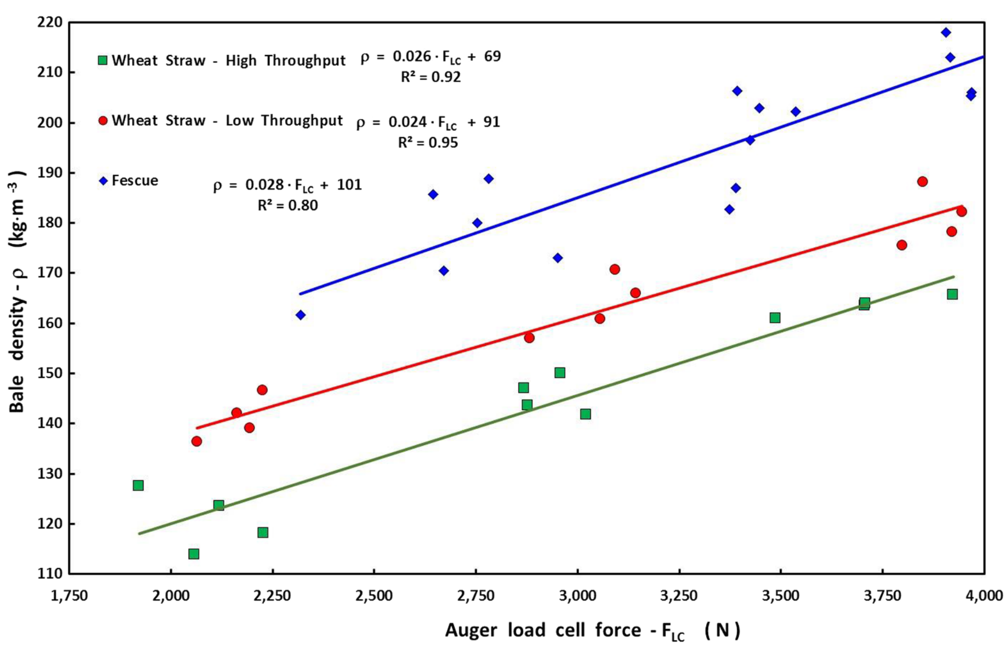

Fig. 9. Average auger load cell force (F_{LC} (N)) for individual bales versus dry basis bale density (ρ (kg·m^{-3})) for two different crops. Auger force was 8.46 times auger load cell force. Throughput for each crop is found in Table 2.

compression panel pressure setpoint to rise to the maximum (Fig. 8, B) which eventually caused the auger force to overshoot its setpoint. The compression panel pressure reacted to this and eventually the auger force was controlled around its setpoint. When the bale length was reached and the separation arms entered the bale chamber, the auger force would rise as incoming material packed against the separation arms (Fig. 8, C). When the bale separation arms were in the bale chamber, the auger force control loop was paused (Fig. 8, D) to prevent

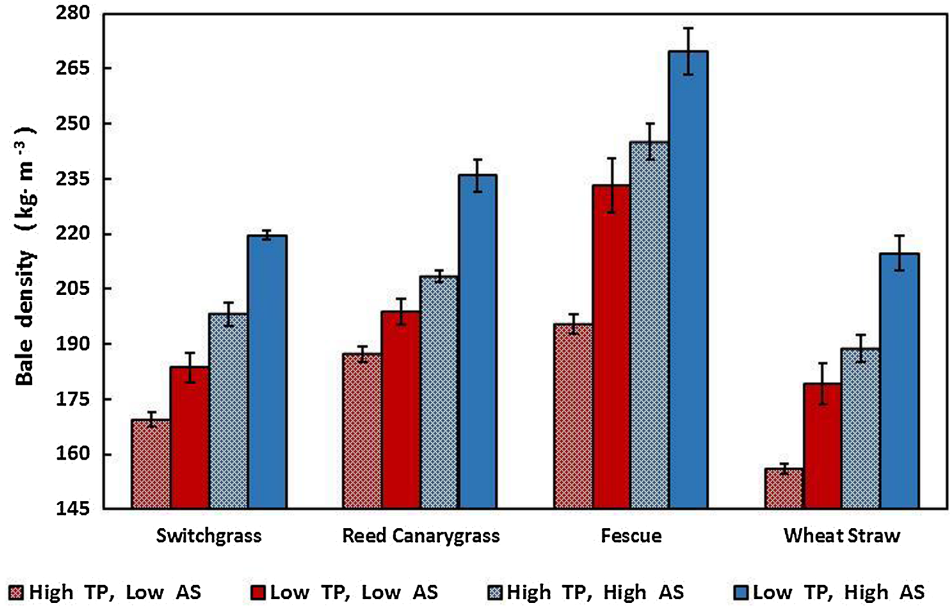

Fig. 10. Dry basis bale density at different throughputs (TP) and auger speeds (AS). Throughputs and auger speeds are found in Table 3. Error bars represent SEM.

Table 4
Predicted dry basis bale density at various plunger loads for a conventional large-square baler based on data from Shinners and Friede (2018).

Approximate plunger force[a] (kN)	Dry basis bale density ($kg \cdot m^{-3}$) Switchgrass	Wheat Straw	Corn Stover
140	140	100	110
280	180	125	145
420	210	150	175
560	230	165	195
700	250	180	215

[a] Approximate plunger load using conventional large-square baler based on maximum plunger load of 700 kN for baler tested. See Shinners and Friede (2018).

the compression panel pressure from dropping excessively when responding to the elevated auger force. When the baler was traveling across the headlands during a turn, and little to no material was being gathered by the baler, the control system was paused to maintain the pressure in the compression panel cylinders. However, to ensure that the control system was not improperly paused when throughput was very low when baling, a threshold speed for bale movement through the chamber was set to avoid pausing in a light windrow. This caused the panel pressure to rise slightly when throughput dropped but before control could be paused. During these events the auger force dropped, bale length was relatively constant and the compression panel setpoint increased (Fig. 8, E and F).

During preliminary tuning of the PID terms, the range of absolute error of the auger force was typically 17% to 20% (data not presented). After these preliminary tests and before the first experiment, additional tuning was conducted so that during the first experiment the range of absolute errors was 3% to 15% with an average of 9% (Table 2). Additional tuning after the first experiment reduced the absolute error to 1% to 7% with an average of 3% during the second experiment (Table 3). The magnitude of the error was not well correlated with the auger force setpoint.

Dry basis bale density was linearly correlated with auger force which indicated that using the auger force setpoint to target a desired bale density was appropriate (Fig. 9). The relatively small SEM for bale density (Tables 2 and 3) shows that the control system was creating consistent bale to bale density. Bale density decreased as auger force decreased or as throughput increased (Table 2, Fig. 9). It was hypothesized that the compression energy per unit mass controls the subsequent bale density. This can be controlled by either decreasing the mass under the rollers at a given time by increasing auger speed which creates a thinner layer laid on the bale face or by increasing the energy being put into that mass by increasing the auger force. Results from the first experiment showed that increasing the auger force could overcome the reduction in bale density caused by greater throughput (Table 2, Fig. 9). Results from the second experiment showed that operating the auger at 167 rpm during high throughput tests resulted in greater bale density than when the auger speed was 90 rpm during low throughput tests (Table 3, Fig. 10). These results suggest that to achieve a desired bale density it could be beneficial to develop new baler mechanical and control systems to vary both auger force and auger speed based on crop type and throughput.

The maximum throughput obtained with the ABer was about half of what would be expected from a conventional plunger baler of similar bale size. The results show that as throughput increases auger force and speed may need to be greater to achieve a desired bale density. Also, as throughput increases, a greater mass of material would be pushed against the separation arms during bale separation and tying. To prevent potential plugging or excessive auger force during bale separation at greater throughputs would require decreasing the bale separation arms cycle time from the current value of 12 s. Further research would be required to investigate the effect on baler power requirements of increasing auger force and speed and decreasing separation arm cycle time through greater hydraulic flow.

Manufacturers offer LSBers which produce bales of varying density based on applied plunger forces (AGCO, 2017). Previously published bale density data for crops baled at various LSBer plunger forces was used for comparison with density of bales formed by the ABer (Table 4). At 25 to 30 kN of applied force at the auger, the ABer produced bale densities that were comparable to a LSBer applying 300 to 700 kN (Tables 2–4). However, throughputs of the LSBer were two to three times that of the ABer (Shinners and Friede, 2018). Future research is required to determine if an ABer which varies both auger force and speed can produce bale densities comparable to a LSBer when both are operated at similar throughputs.

Future changes to improve the performance of the baler control system could include reductions in the delay when the control system was paused when there was very slow growth in bale length. This would prevent over tensioning the bale chamber as auger force drops during headland turns or during very low throughputs. Even though the compression panel control was paused during bale separation, the delay between the arms returning to the home position and crop filling that void causes the panel pressure to increase and auger force to overshoot. Adding in an appropriate delay after the arms have returned home and when compression panel control resumes might help alleviate this issue. It would be appropriate to develop settings and vary performance based on the type of crop being harvested. This would allow for more aggressive changes in compression panel pressure for easily compressible/low friction crops (i.e. straw) and less aggressive response for crops that are prone to plugging (i.e. alfalfa). Additionally, if the ABer would be powered by a tractor with CVT transmissions for both the ground and PTO drives, then a tractor-implement automation system could link auger and ground speed to create layer thicknesses that optimizes bale density and auger force.

6. Conclusions

A new concept large-square baler was developed which used continuous compaction with an auger and conical compaction rollers to compress material as it is placed on the bale face. The closed-loop control system used auger force and bale chamber compression panel pressure to control bale density, which was linearly related to auger force. The system also controlled the bale separation and tying process when the desired bale length was reached. Tuning of the PID terms reduced the absolute error of the auger force to an average of 3%. Bale density comparable to that typically produced with a conventional baler was created with much lower forces, which could help reduce the cost of creating high-density bales.

Acknowledgements

This research was partially sponsored by the University of Wisconsin College of Agriculture and Life Sciences; and CenUSA, a research project funded by the Agriculture and Food Research Initiative Competitive Grant No. 2011-68005-30411 from the USDA National Institute of Food and Agriculture. We also gratefully acknowledge the financial, material and technical support of John Deere Ottumwa Works, Digi-Star International, and Weasler Engineering.

References

ASABE, 2012. S358.2: Moisture measurement-Forages. ASABE, St. Joseph, MI.
AGCO, 2017. Introducing the square baler classification system. Retrieved from http://hesston.com/therightbaler/pdf/HS17P002CR-Square-Baler-Class-Flyer-LR.pdf.
Flick, D.E., 2018. Innovative Methods for Densification and Storage of Biomass Crops. Master of Science Thesis, Department of Biological Systems Engineering. University of Wisconsin.
Kenney, K.L., Hess, J.R., Stevens, N.A., Smith, W.A., Bonner, I.J., Muth, D.J., 2014. Biomass logistics. Bioprocess. Renew. Resourc. Commod. Bioprod. 29–42.
Miao, Z., Phillips, J.W., Grift, T.E., Mathanker, S.K., 2013. Energy and pressure requirement for compression of Miscanthus giganteus to an extreme density. Biosyst. Eng. 114 (1), 21–25.
McAfee, J.R., Shinners, K.J., Friede, J.C., 2018. Twine-tension in high-density large-square bales. Appl. Eng. Agric. 34 (3), 515–525.
Ozderya, H.Y., 2017. SerialPlot V10.0 https://hackaday.io/project/5334-serialplot-realtime-plotting-software/discussion-88924 Accessed March, 2019.
Shah, A., Darr, M., 2016. A techno-economic analysis of the stover feedstock supply system for cellulosic biorefineries. Biofuels, Bioprod. Biorefin. 10 (5), 542–559.
Searcy, E.M., Hess, J.R., 2010. Uniform-format feedstock supply system: A commodity-scale design to produce an infrastructure-compatible biocrude from lignocellulosic biomass. EXT- 1020372. Idaho National Laboratory.
Sibley, D.L., Sibley, D.A., 1995. Apparatus for baling bulk fibrous material. US Patent No. 5,377,481.
Siebenga, C., 2013. Continuous square baler. US Patent No. 2014/0123862 A1.
Shinners, K.J., Friede, J.C., 2018. Energy requirements for biomass harvest and densification. Energies 11 (4), 780.